PERGAMON

Chemical Engineering Science 56 (2001) 2459–2473

Chemical Engineering Science

www.elsevier.nl/locate/ces

Influence of different scales of mixing in reaction crystallization

Marika Torbacke, Åke C. Rasmuson*

Department of Chemical Engineering and Technology, Royal Institute of Technology, S-100 44 Stockholm, Sweden

Abstract

Experiments on semibatch reaction crystallization of benzoic acid are reported. The conditions in an agitated tank are simulated by a loop reactor by which feed point mixing conditions can be controlled separately from the macroscale circulation rate. Hydrochloric acid is fed into a circulating solution of sodium benzoate and the influence of macromixing, mesomixing and micromixing on the product crystal mean size is evaluated. The product mean size increases with increasing circulation rate in the loop, with increasing feed point mixing intensity, with decreasing feed rate and with decreasing feed pipe diameter. Increased mixing intensity on any level leads to larger product crystals, but especially the rate of mesomixing is of importance. The influence of the feed pipe diameter is opposite to predictions by available theories and cannot be explained by backmixing into the feeding pipe. All results can be correlated quite well against a dimensionless mixing efficiency defined as the ratio of the reactant feeding time to the mixing time. The mixing time is the sum of the time constants for mesomixing and micromixing. A new mesomixing time constant is defined as being proportional to the ratio of the feed pipe diameter and the velocity of the bulk flow passing the feed pipe. © 2001 Published by Elsevier Science Ltd.

Keywords: Reaction crystallization; Precipitation; Benzoic acid; Macromixing; Mesomixing; Micromixing; Semibatch; Loop reactor; Backmixing; Colour experiments

1. Introduction

Reaction crystallization is commonly used in production of some inorganic compounds like calcium carbonate and barium sulphate, but is also extensively used in production of pharmaceuticals and organic fine chemicals. In these latter processes, often one reactant solution is fed into an agitated solution of the other reactant in semibatch operation. The chemical reaction is often fast and the solubility of the product compound is from moderate to very low compared to reactant concentrations. Hence, the supersaturation at the feed point becomes high and the process proceeds under conditions of segregation. If also the rates of nucleation and crystal growth are high the mixing conditions will influence the product size distribution significantly.

Research shows that the agitation rate, the feed point mixing intensity and the feed rate affect the product size distribution. A review over semibatch studies are given in Tables 1 and 2. Most studies are concerned with precipitation of inorganic compounds forming ionic crystals, and the influence of process parameters are somewhat diverging. Commonly, the crystal size is found to decrease with increasing feed rate in single-feed semibatch experiments. The influence of the feed pipe diameter is not much studied in reaction crystallization.

Åslund and Rasmuson (1992) studied semi-batch precipitation of benzoic acid by adding hydrochloric acid to a sodium benzoate solution in a stirred-tank reactor. The influence of agitation rate, agitator type and feed point location could be well correlated by the estimated feed point energy dissipation rate. The product weight mean size initially increases with increasing local energy dissipation rate, reaches a maximum, and then decreases again. In addition, larger crystals are produced with a decreased feed rate and decreased reactant concentrations. In explaining the results, several different rate processes have to be acknowledged. The solubility is much lower than reactant solution concentrations, and the acid–base reaction is very fast. Hence, the local supersaturation at the feed point becomes very high, leading to rapid nucleation and crystal growth. From the very high value at the feed point, the supersaturation decays when the solution is conveyed into the bulk. Mixing in the stirred-tank reactor brings reactants together on the one hand, but may also act to dilute local concentrations.

* Corresponding author. Tel.: +46-8-7908227; fax: +46-8-105228.
E-mail address: rasmuson@ket.kth.se (Å. C. Rasmuson).

0009-2509/01/$ - see front matter © 2001 Published by Elsevier Science Ltd.
PII: S0009-2509(00)00452-8

Table 1
The effect of the string rate or energy dissipation on the mean crystal size[a]

Effect	Single or double feed	Substance	Reference
∩	Double	Silver bromide	Muhr, David, Villermaux, and Jezequel (1995)
↓	Double	Silver chloride	Stavek, Fort, Nyvlt, and Sipek (1988)
∩ and ∪	Double	Barium sulphate	Tosun (1988)
↑ and _	Double	Barium sulphate	Podgorska, Baldyga, and Pohorecki (1993) Baldyga, Podgorska, and Pohorecki (1995)
↓	Double	Calcium oxalate	Marcant and David (1993) David and Marcant (1994)
∩ and ∪	Double	NiDMG	Kuboi, Harada, Winterbottom, Anderson, and Nienow (1986)
∩	Single	Benzoic acid	Åslund and Rasmuson (1992)
∩	Single	Calcium oxalate	Marcant and David (1991)
∩ or _	Single	Calcium oxalate	Marcant and David (1993)
↑	Single	Calcium oxalate	Houcine, Plasari, David, and Villermaux (1997)
∩ and ∪	Single	Barium sulphate	Chen, Zheng, and Chen (1996)
∩ and ∪	Single	Barium sulphate	Philips, Rohani, and Baldyga (1999)
∪	Single	Barium sulphate	Tosun (1988)
↓	Single	Barium sulphate	Tovstiga and Wirges (1990)
↓	Single	Barium sulphate	Baldyga, Pohorecki, Podgorska, and Marcant (1990)
∩	Single	NiDMG	Kuboi et al. (1986)

[a] ∩ = maximum; ∪ = minimum; ↑ = increase; ↓ = decrease; _ = no clear influence (constant).

Table 2
The effect of the feed rate on the mean crystal size in semibatch processes[a]

Effect	Single or double feed	Substance	Reference
↓	Double	Silver bromide	Muhr et al. (1995)
↓ or –	Double	Barium sulphate	Podgorska et al. (1993) Baldyga et al. (1995)
↓	Single	Cadmium sulphide	Ramsden (1985)
↓	Single	Barium sulphate	Philips et al. (1999)
–	Single	Barium sulphate	Tovstiga and Wirges (1990)
↓	Single	Barium sulphate	Chen et al. (1996)
↓	Single	Benzoic acid	Åslund and Rasmuson (1992)
↓ or –	Single	Calcium oxalate	Marcant and David (1993)

[a] Keys as in Table 1.

Macroscopic circulation brings supersaturation and crystals back to the feed point. Small nuclei generated at the feed point are conveyed by macromixing into the bulk and may dissolve due to Ostwald ripening. In addition, in a semibatch process the reactant in the agitated solution is continuously consumed throughout the process. The maximum product supersaturation is gradually reduced and the size distribution of the suspension changes over the process time. Furthermore, the hydrodynamic situation in an agitated tank is quite complex in itself with strong spatial variations in flow and mixing intensity. Because of this complexity, the results obtained by Åslund and Rasmuson (1992) were difficult to explain fully.

The hydrodynamics of a stirred tank varies from location to location, both in terms of micromixing and in terms of macromixing. The rate of micromixing depends on the local rate of dissipation of the turbulent energy and is sensitive to the exact location especially in the impeller region. With an axial flow agitator liquid circulates in a macroscale loop in the stirred tank. The circulation rate is not uniform, but should rather be described by a circulation rate distribution. A change in agitation rate changes the energy dissipation rate and the linear flow velocity at the feed point, as well as the overall circulation time. Hence, the importance of different levels of mixing are difficult to resolve from agitated-tank experiments.

In the present study, the agitated-tank crystallizer is simulated experimentally by a loop reactor. The liquid circulates around a loop in the loop reactor, like the circulation loop in an agitated tank. However, the circulation time is well-defined and easily controlled. One reactant is added through a feed pipe and a second agitator, in front of the feed pipe, is used to separately control the feed point micromixing intensity.

By changing the feed pipe diameter mesomixing is varied. Thus, all levels of mixing — macromixing, mesomixing and micromixing — can be controlled independently of each other. An extensive series of experiments on semibatch crystallization of benzoic acid is presented. The influence of macromixing, mesomixing and micromixing on the product weight mean size is investigated, and the results are compared with current mixing theories.

2. Experimental work

2.1. Apparatus

The loop reactor (Fig. 1) is manufactured from a glass pipe of 45-mm inner diameter. The total length of the loop is 1.05 m. An expansion vessel is attached to the loop reactor to allow for volume changes during the semibatch process. There is a 35-mm diameter marine propeller stirrer in one of the legs working as a circulation pump (Fig. 2). The propeller stirrer is pumping downwards and is fitted 8–10 cm down from the transverse pipe. The feed is added through a glass pipe using a two-piston pump. The feed pipe is connected to the pump-Teflon-hose with Swagelok® tube fittings. Different feed pipes have been used with the inner diameters of 0.7, 1.5, 2.5 and 3.9 mm. These feed pipes are straight and have a circle-shaped cross-section. In a few experiments two other feed pipe designs have been explored: one with a circular cross-section and 0.7 mm i.d., but being bent 90° and one straight with a rectangular 1.4×3 mm cross-section. In front of the feed pipe, inside the loop reactor, a 25-mm Rushton turbine is used to control feed point mixing. The turbine impeller is located 5 mm away from the feed pipe outlet in all experiments regardless of feed pipe design. Therefore, the vertical position of the turbine impeller differs somewhat between experiments. For example, when the bent feed pipes are used, the vertical location of the turbine is slightly adjusted making the feed pipe outlet location with respect to the turbine unaltered. A paddle stirrer is placed in the expansion volume to avoid sedimentation of benzoic acid crystals.

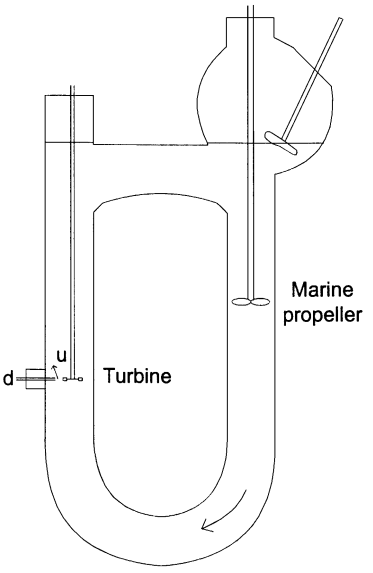

Fig. 1. The loop reactor.

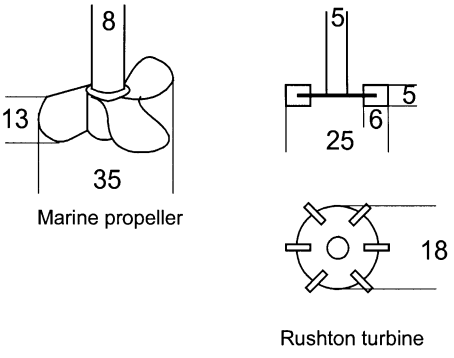

Fig. 2. The agitators.

2.2. Procedures

In all experiments 483 ml of 1.4 M hydrochloric acid is added to a 1930 ml solution of 0.35 M sodium benzoate at 30.0°C in the loop reactor. At the end of each experiment the amount of added hydrochloric acid is stoichiometric to the initial amount of sodium benzoate. The initial sodium benzoate solution in the reactor is saturated with benzoic acid and contains a stoichiometric amount of sodium chloride. The total feed time is in general 90 min. However, in some experiments the total feed time is either 30, 45 or 180 min. The linear feed velocity varies from 0.007 m/s (3.9 mm i.d., 90 min experiment) to 0.7 m/s (0.7 mm i.d., 30 min experiment). The feed pipe flow is laminar since the Reynolds number ranges from 27 to 470. The propeller stirring rate is generally 600 rpm. However, in some experiments the propeller stirring rate is 450, 750 or 900 rpm. The turbine stirring rate is in general 75 rpm. However, in some experiments the turbine stirring rate is either 300,500,700 or 1100 rpm. Usually, two samples of 20 ml are withdrawn from the suspension in the loop reactor at the end of each experiment. Three droplets of dispersing agent are added to each sample. Åslund and Rasmuson (1992) found that the aggregate size distributions do not correlate with changes in the process variables like the crystal size distributions do. Therefore, a sample is run three times for 5 s each in an ultrasonic bath in order to disintegrate aggregated crystals. A weighed amount of the disintegrated sample is withdrawn with a blunted Pasteur pipette, a sub-sample, and is added to the thermostated electrolytic solution. Two sub-samples are in general taken from each sample. The electrolytic

solution contains sodium chloride and has previously been saturated with benzoic acid. The crystal size distribution is determined with an electrosensing zone instrument (ELZONE® 180 XY) for each sub-sample. An orifice tube of either 150 or 300 μm is used for the measurements. The volume measured each time is either 2.00 or 5.01 ml.

From each analysis a weight mean size is calculated from the mass density distributions obtained. In general, the weight mean size from the analyses of the two sub-samples from the same sample differ less than 2 μm, and the same range holds in general for sub-samples from different samples. The weight mean size presented in the results and the discussion, is the averaged value of all the sub-samples from each experiment. Many experiments have been repeated once. Typically, the averaged weight mean size differ no more than 1 μm between reproducibility experiments. One experiment has been repeated twice (1.5 mm, 600 rpm propeller, 75 rpm turbine, and 90 min), and the averaged mean sizes were 37.9, 36.6 and 36.9 μm. In those cases where the experiment has been repeated, an average over all sub-samples from all experiments is used in the result presentation and the discussion.

The shape and the size of the particles are noted under a microscope for each sample. When the propeller stirring rate is low (450 rpm) the shape of the crystals is somewhat irregular (Fig. 3). Some crystals are cauliflower-shaped. Most crystals are platelet-shaped, and are even in shape and size. With a 600 rpm propeller stirring rate the crystals are all shaped as platelets with rounded (not broken) corners. Some crystals are small and round-rectangle shaped. The larger crystals are broken, especially in the corners. At 750 rpm propeller stirring rate the crystals are even more broken. At 900 rpm propeller stirring rate, the crystals have less rounded corners, and are more broken. The small crystals are even in shape, while the larger crystals are platelets with broken corners and edges. The largest particles are intact, but torn. The crystals are more broken at higher turbine stirring rates than at lower stirring rates. When the turbine stirring rate is increased to 700 rpm the crystals appear very rugged. Some crystals are very small and unevenly shaped. Other crystals are medium sized and platelet-shaped with broken corners and edges. The largest crystals are rugged and shapeless.

The hydrodynamics in the loop reactor was studied by first adding a coloured pH indicator, methyl orange, to water circulating in the loop. After that a hydrochloric acid pulse is added through the feed pipe. The colour changes from colourless/yellow to red with decreasing pH. The coloured acid pulse is well mixed in the propeller region, thus, forming a coloured front leaving the impeller region. This coloured front was clocked for different propeller stirring rates and volumes in the loop reactor. The linear velocity depends linearly on the propeller stirring rate, and it varies from 0.07 to 0.48 m/s when the marine propeller stirring rate is varied from 200 to 900 rpm. The linear velocity is independent of the volume changes during each experiment (Torbacke, 1998) and is not affected by turbine stirring rates of 700 rpm or lower. Macroscale circulation times (Table 5) are calculated from the linear velocity measurements knowing that the length of the loop reactor is 1.05 m. Experiments are run for propeller stirring rates ranging from 450 to 900 rpm for which the pipe flow Reynolds number in the loop varies from 9900 to 21,600.

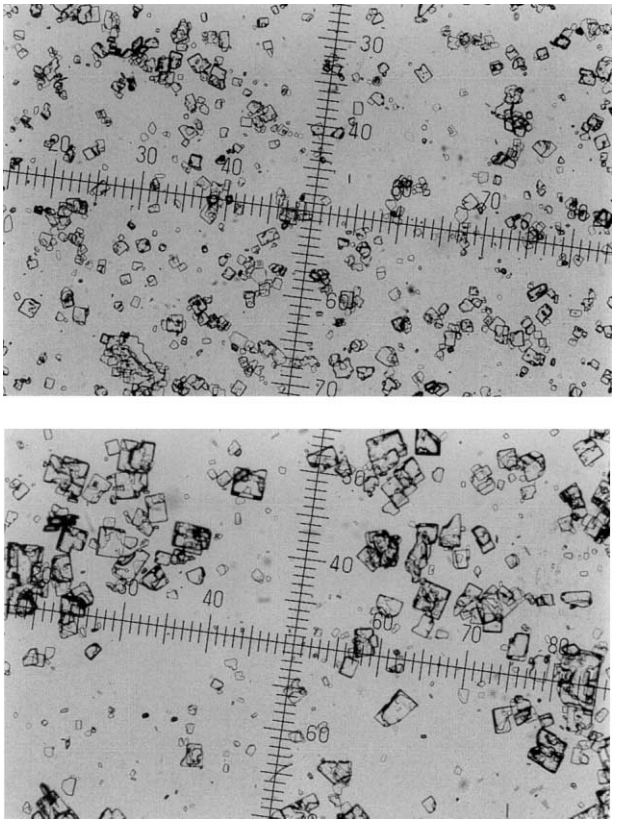

Fig. 3. The benzoic acid crystals from low mixing intensity experiment ($N_{prop} = 450$ rpm, $N_{turb} = 75$ rpm) (top) and high mixing intensity experiment ($N_{prop} = 900$ rpm, $N_{turb} = 700$ rpm) (bottom).

2.3. Results

A few examples of product size distributions, at different total feeding times, are given in Fig. 4 as relative mass density distributions. The relative mass density is defined as the crystal mass in a size interval divided by the total mass of crystals and the size interval, ΔL_i. The crystal size obtained from the particle counter is given as the volume-equivalent spherical diameter. The result presentation focus on the product weight mean size which is estimated as (Randolph & Larson, 1988):

$$L_{43} = \frac{\sum N_i L_i^4}{\sum N_i L_i^3}, \tag{1}$$

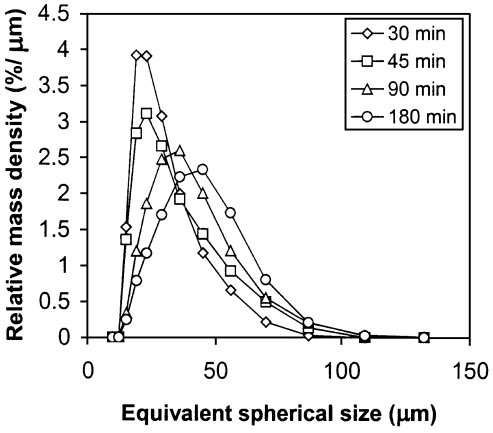

Fig. 4. Product size distributions, $d = 0.7$ mm.

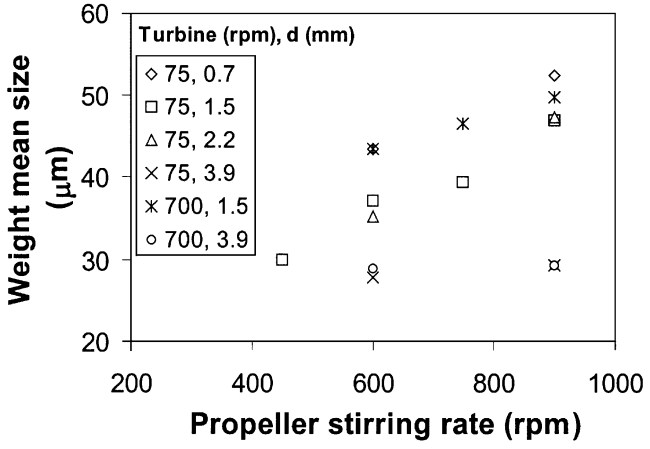

Fig. 5. Influence of micromixing, $t_f = 90$ min.

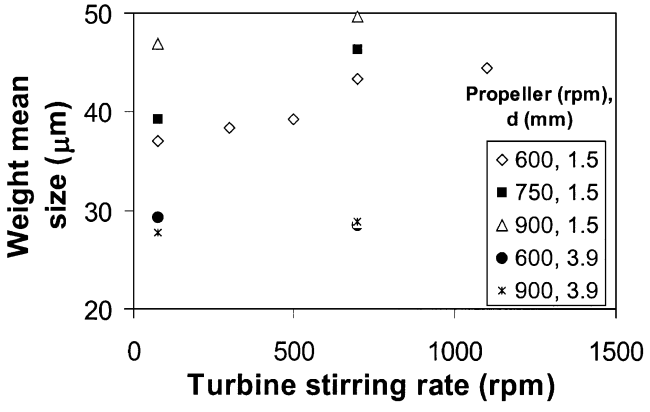

Fig. 6. Influence of macromixing, $t_f = 90$ min.

where N_i is the number of particles in a size interval and L_i is the arithmetic mean size of the same interval.

Fig. 5 shows the influence of the macroscale circulation rate in the loop. The weight mean size clearly increases with increasing propeller stirring rate except for the 3.9 mm feed pipe. Fig. 6 shows the influence of the feed point mixing intensity. For the 1.5 mm feed pipe diameter,

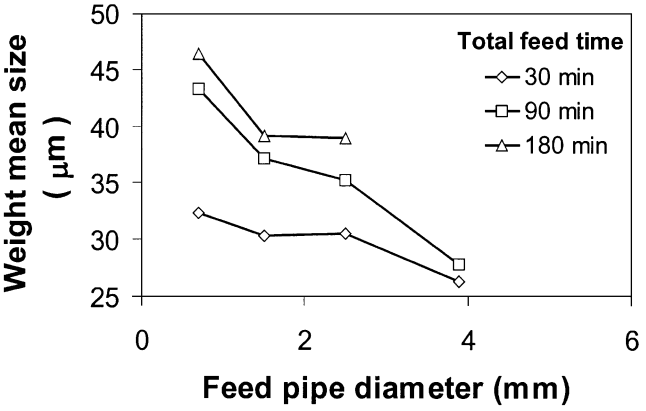

Fig. 7. Influence of mesomixing, $N_{prop} = 600$ rpm and $N_{turb} = 75$ rpm.

the weight mean size increases with increased turbine agitation rate regardless of the level of macroscale circulation. However, for the 3.9 mm feed pipe diameter there is no influence of feed point mixing intensity. The influence of the feed pipe diameter and the total feeding time are shown in Figs. 7 and 8, respectively. The mean size increases with decreasing feed pipe diameter. In addition, the mean size increases with reduced feed rate, but this increase tends to level off at longer feeding times.

The influence of changing the feeding direction and the shape of the feed pipe is shown in Fig. 9. In the previous diagrams the feed pipes have circular cross-section and the feeding direction is perpendicular to the axis of the loop and the overall bulk flow. From the experiments with the 0.7 mm diameter feed pipe bent 90°, either pointing upwards or downwards, we find no significant influence of the feeding direction (Fig. 9). However, compared to the standard feed pipes at equal cross-sectional area, the feed pipe having a rectangle-shaped cross-section, produce a product having a significantly increased mean size (Fig. 9). The rectangle-shaped feed pipe is used in two different orientations — either with the longest side turned along the direction of the overall bulk flow or with the longest side perpendicular to the overall bulk flow. No significant influence of the rectangle-shaped feed pipe orientation is found.

3. Evaluation

Often the influence of mixing in reaction crystallization in agitated tanks is discussed in terms of the turbulence energy dissipation rate (Åslund & Rasmuson, 1992), and in particular the turbulence energy dissipation rate at the feed point. The energy supplied by the agitators is as a first estimate calculated as

$$P = N_p N^3 D^5 \rho, \tag{2}$$

where N_p is the power number, N is the stirring rate, D is the impeller diameter, and ρ is the density of the

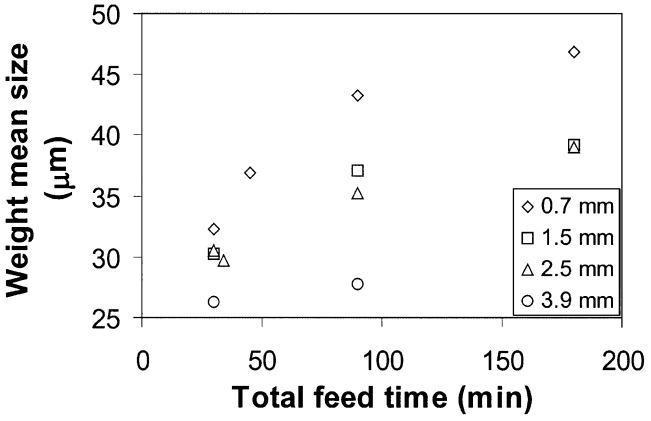

Fig. 8. Influence of total feeding time, $N_{prop} = 600$ rpm and $N_{turb} = 75$ rpm.

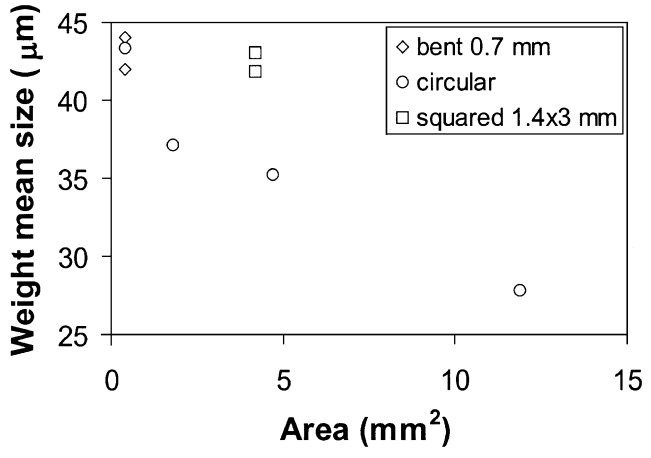

Fig. 9. Influence of feed pipe cross-sectional area, $N_{prop} = 600$ rpm and $N_{turb} = 75$ rpm. $t_f = 90$ min.

suspension. The propeller impeller Reynolds number ranges from 9000 to 18,000, and the turbine impeller Reynolds number ranges from 780 to 11,500. The pipe flow Reynolds number in the loop is well in the turbulent region. Hence, appropriate power numbers cannot be defined easily. For a first rough estimation, the power number is taken as 0.5 for the propeller stirrer and 5 for the turbine stirrer (Nienow, 1985; Oldshue, 1983; Rushton, Costich, & Everett, 1950) even though these values have been determined for baffled agitated tanks in the turbulent region. The final volume in the loop reactor is 2420 ml, which is converted to a mass assuming the density of water. This mass is used in the mean energy dissipation rate calculations for both the turbine and the propeller impeller contributions.

The local feed point mixing intensity is determined by the turbine agitation rate, the propeller agitation rate and the feed flow rate. In all experiments the feed pipe flow is laminar and the kinetic energy of the feed stream is negligible compared to the mixing energy of the agitation. The contribution from the propeller stirrer at the feed point is assumed to be equal to the level of dissipation in the bulk region in a corresponding stirred tank. In estimating the local energy dissipation rate at the feed point we use half the mean specific power input furnished by the marine propeller (Franke & Mersmann, 1995). The turbine agitator energy dissipation is assumed to be concentrated to a more reduced volume. This volume is estimated by studying a decolourisation reaction when acid is added through the feed pipe into the loop reactor. The feed point is positioned in the turbine impeller discharge. The vertical distance around the turbine stirrer where the decolourisation takes place is roughly measured, and is converted to a volume by multiplication with the cross-sectional area of the loop reactor. This volume is approximately 30 ml for all turbine stirring rates, and the value is used in the calculation of the mean specific power input of the turbine. The feed point is always located in the intensively mixed outflow from the turbine agitator and the energy dissipation rate contribution from the turbine is taken as 15 times the corresponding mean specific energy dissipation rate (Geisler, 1991). The total feed point energy dissipation rate resulting from these two contributions is given in Table 3. Obviously, at the feed point the micromixing intensity is almost completely governed by the turbine agitation.

Table 3
The local energy dissipation rate in the feed region

Turbine stirring rate	450 rpm propeller	600 rpm propeller	700 rpm propeller	900 rpm propeller
75 rpm	0.050 W/kg	0.053 W/kg	0.058 W/kg	0.066 W/kg
700 rpm		38.77 W/kg	38.78 W/kg	38.79 W/kg

Product weight mean sizes are plotted versus the feed point energy dissipation rate in Fig. 10. As shown, the mean size increases with increasing local energy dissipation rate, but there are major features of the results that cannot be satisfactorily explained by this parameter. Results from experiments with different feed pipe diameters, different total feed times and different propeller stirring rates but constant turbine impeller stirring rate, are vertically aligned in Fig. 10. At constant low level of feed point micromixing the weight mean size increases from 30 to 47 μm with increasing rate of propeller agitation. The weight mean size increases from 26 to 46 μm when changing the feed pipe diameter. At high level of turbine agitation, the weight mean size increases from 43 to 50 μm at increasing propeller agitation. The weight mean size increases from 29 to 46 μm when changing the feed pipe diameter. The local energy dissipation rate can neither explain the influence of the feed pipe diameter nor of the propeller agitation rate, since the feed point micromixing is almost completely governed by the turbine agitation. The contributions of the kinetic energy of

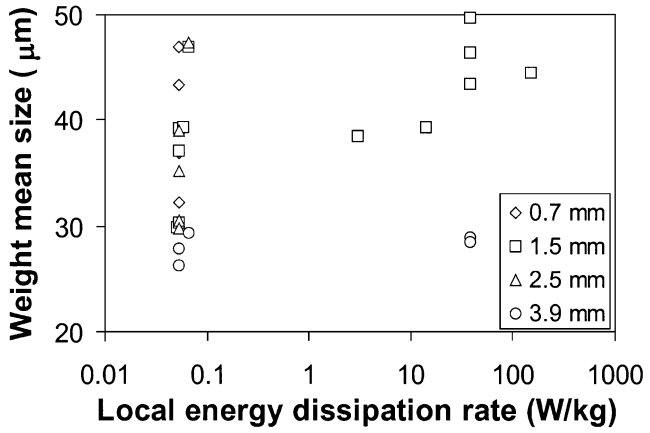

Fig. 10. Correlation of mean size to the feed point specific energy dissipation rate.

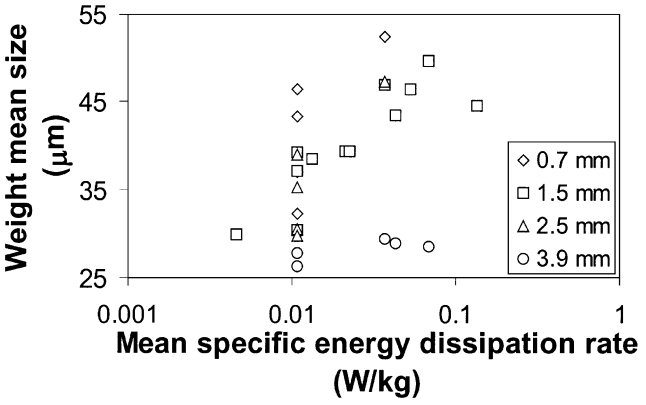

Fig. 11. Correlation of mean size to the average specific energy dissipation rate.

Table 4
The calculated total mean specific power input in the loop reactor at different stirring rates (propeller/turbine)

Stirring rates (propeller/turbine) (rpm)	$\varepsilon_{\text{Loop Reactor}}$ (W/kg)
600/0	0.0108
450/75	0.0046
600/75	0.0108
750/75	0.0212
900/75	0.0368
600/700	0.0429
750/700	0.0532
900/700	0.0686

Table 5
The circulation times and resultant velocities in the loop reactor

N_{prop} (rpm)	N_{turb} (rpm)	u_b (m/s)	u_{res} (m/s)
450	75	0.22	0.23
600	75	0.30	0.31
600	300	0.30	0.39
600	500	0.30	0.50
600	700	0.30	0.64
600	1100	0.18[a]	0.90
750	75	0.39	0.39
750	700	0.39	0.69
900	75	0.48	0.48
900	700	0.48	0.74

[a] In these experiments the linear bulk velocity is affected by the turbine agitation.

the feed as well as of the propeller agitation, are quite small.

In case the process is governed by macromixing instead of micromixing the average energy dissipation rate is a better parameter for correlating the results. The average energy dissipation rate is calculated by summation of the power input from the two agitators (Eq. (2)) and dividing by the entire volume in the loop. At 75 rpm turbine stirring rate the turbine contribution to the mean specific power input is negligible. At 700 rpm turbine stirring rate the contribution is approximately equal to that of the propeller agitation at 750 rpm (Table 4). All results are plotted versus the mean specific power input in Fig. 11. The crystal weight mean size increases with increasing average specific energy dissipation rate, but this parameter cannot fully capture the effect of the turbine agitation. For a circulation time of 3.5 s, i.e. 600 rpm propeller stirring rate, the weight mean size increases from 37 to 43 μm with increasing turbine agitation. In addition, the average energy dissipation rate cannot explain the effect of the feed pipe diameter. Experiments with different feed pipes and different total feed times are vertically aligned in Fig. 11.

Alternatively, the linear macroscale circulation velocity can be used to characterise the macromixing. This velocity varies linearly with the rate of rotation of the marine propeller. The correlation with the product weight mean size is however, unsatisfactory. The macroscale circulation velocity is not affected by turbine stirring rates of 700 rpm and below. However, the tangential and the radial velocity of the flow passing the outlet of the feed pipe, increases with increasing turbine agitation. A resultant velocity is calculated (in Table 5) in order to describe the velocity of the flow passing the feed pipe outlet:

$$u_{\text{res}} = \sqrt{u_r^2 + u_t^2 + u_b^2} = \sqrt{(0.53\pi N_{\text{turb}} D_{\text{turb}})^2 + (0.33\pi N_{\text{turb}} D_{\text{turb}})^2 + u_b^2}. \quad (3)$$

The velocity contribution from the turbine impeller, u_r and u_t, is approximated by the mean radial and mean tangential velocities at the location of the feed (Lee & Yianneskis, 1998; Wu & Patterson, 1989). It is assumed that the velocity contribution from the turbine impeller is

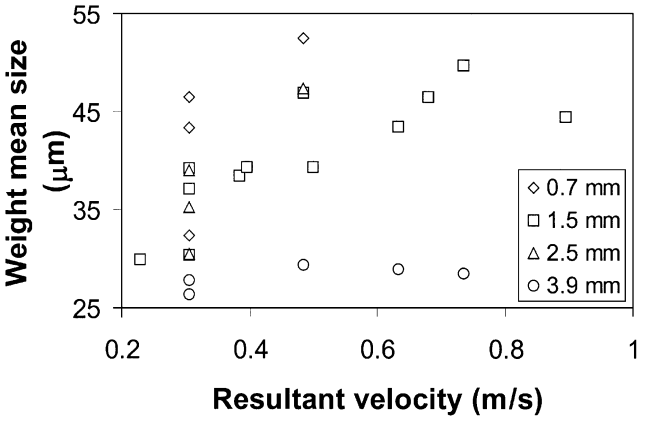

Fig. 12. Correlation of mean size to the resultant velocity of the flow passing the feed point.

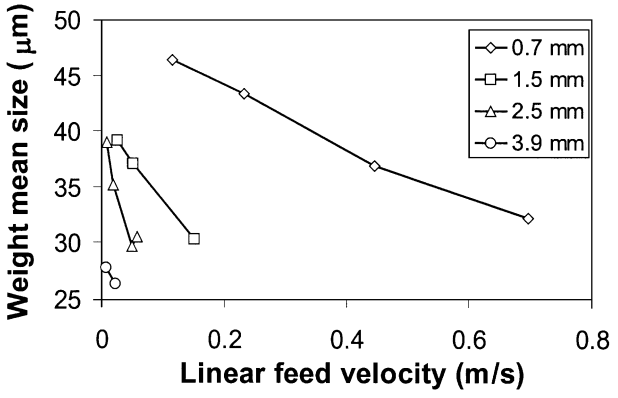

Fig. 13. Influence of the linear feed flow velocity.

perpendicular to the measured circulation velocity in the loop reactor, u_b, created by the propeller impeller. Fig. 12 shows the correlation between the product weight mean size and the resultant linear velocity as calculated by Eq. (3). The correlation is better than a correlation with u_b only, but it is still far from satisfactory. The resultant velocity cannot fully capture the influence of the turbine stirring rate on the mean size and of course not the influence of the feed pipe diameter.

If the linear velocity of the feed reactant in the feed pipe is increased by increasing the volumetric feeding rate, there is a very nice straight line with a negative slope for each feed pipe diameter (Fig. 13). However, if the feed pipe linear velocity is increased by decreasing the feed pipe diameter the effect is the opposite; the mean size increases with decreasing feed pipe diameter at constant volumetric feed rate. Hence, the linear feed pipe velocity does not seem to be the key parameter describing this part of the results. We may also note that the straight lines in Fig. 13, necessarily lead to the levelling off of the curves in Fig. 8 at long feeding times, i.e. at reduced volumetric feed rates.

4. Discussion

The presented experimental results clearly show that the product weight mean size is strongly influenced by the macroscale circulation rate, the feed point mixing intensity, the feed pipe diameter and the feeding rate. The influence of these process variables can be summarised by the more efficient the mixing of the feed with the bulk the larger the product mean size. Increased turbine agitation increases the local mixing with the available bulk solution. Increased propeller agitation provides more bulk solution to the feed point region, which can be mixed with the feed. A reduced feed pipe diameter at equal feed volume flow causes the feed to be more efficiently distributed in the bulk solution. Quite often the specific energy dissipation rate at the feed point is, as a first approximation, assumed to describe the influence of mixing in reaction crystallization processes. However, this parameter can neither explain the influence of the macroscale circulation rate nor the influence of the feed pipe diameter in the present experiments. Hence, we must acknowledge that not only micromixing but also mixing at larger scales has an important influence on the product crystal mean size. It is also shown that the influence of process parameters on the product mean size can neither be fully explained by parameters used to describe macromixing. In addition, the very clear influence of the feed pipe diameter shows that mesomixing is of great importance.

4.1. Different scales of mixing

The mean circulation time in all experiments is much shorter than the total feeding time and hence the loop reactor should be assumed to be completely macromixed (Baldyga, Bourne, & Hearn, 1997). Hence, the influence of the macroscale circulation rate, i.e. of the propeller stirring rate, should be regarded as a mesomixing effect rather than a macromixing effect. The mean crystal size increases with increasing feeding time, i.e. with decreasing feed rate, but this influence levels off at long feeding times. The same was found in a previous study performed in an agitated tank (Åslund & Rasmuson, 1992). This is a characteristic feature of a process influenced by mesomixing (Baldyga, Bourne, & Yang, 1993). With decreasing feed rate the relative importance of micromixing to mesomixing increases. The process becomes entirely governed by the rate of micromixing at sufficiently low feed rates, and the influence of the feed rate vanishes. However, this state does not seem to be reached in the present work. The influence of mesomixing in the present study is further manifested by the influence of the feed pipe diameter and the design of the feed pipe.

The characteristic length scale of mesomixing, L_D, is a measure of the rate of dispersion of the feed flow

(Baldyga et al., 1993). It is defined as

$$L_D = \sqrt{\frac{Q_{\text{feed}}}{u}}, \tag{4}$$

where Q_{feed} is the volumetric flow rate of the feed. The linear velocity of the flow passing the feed entrance, u, is calculated by us as the resultant velocity according to Eq. (3). For 30 min total feeding time, 600 rpm propeller agitation and 75 rpm turbine stirring rates, the largest L_D-value is obtained (0.94 mm). The value of L_D decreases to 0.55 mm when the total feeding time increases to 90 min. The lowest L_D-value is obtained (0.32 mm) when the turbine stirring rate is increased to 1100 rpm. We may note that there are larger variations in Q_{feed} than in u in the present work. In all, but one case, L_D is smaller than the feed pipe diameter, and hence the feed should be treated as a local finite source as opposed to a point source (Baldyga et al., 1993).

4.2. Turbulent dispersion

The analysis of mesomixing by turbulent dispersion, describes the radial dispersion of the feed into the surrounding, parallel bulk flow (Baldyga et al., 1993). The problem is solved as a Fick's second law problem with constant diffusivity for the case of a finite cylindrical source. As the feed is dispersed, it expands radially like a truncated cone from the feed pipe outlet. Mesomixing occurs latest along the axis of the cone and is described by

$$X^0_{\text{feed}}(t) = \frac{4Q_{\text{feed}}}{\pi d^2 u}\left(1 - \exp\left(-\frac{d^2}{16D_t t}\right)\right), \tag{5}$$

where X^0_{feed} is the volume fraction of feed solution at a certain time downstream from the pipe along the axis of the cone (denoted by superscript 0), d is the feed pipe diameter, t is the time after the feed has left the feed pipe, and D_t is the turbulent diffusivity. The factor ahead of the parenthesis is the dimensionless number, U:

$$U = \frac{4Q_{\text{feed}}}{\pi d^2 u} = \frac{u_{\text{feed}}}{u}. \tag{6}$$

The argument of the exponential term is transformed into dimensionless parameters according to

$$\frac{d^2}{16D_t t} = \frac{Q}{4\pi T U}, \tag{7}$$

where T is a dimensionless time defined as

$$T = Et, \tag{8}$$

and E is the engulfment rate coefficient (Baldyga & Bourne, 1989)

$$E = 0.058\sqrt{\frac{\varepsilon}{\nu}}. \tag{9}$$

Therefore, mesomixing depends on two dimensionless parameters U and Q (Baldyga et al., 1993). Q is the ratio of the characteristic times for mesomixing and micromixing

$$Q = \frac{\tau_{\text{meso}}}{\tau_{\text{micro}}}. \tag{10}$$

The characteristic mesomixing time is determined as (Baldyga & Bourne, 1992)

$$\tau_{\text{meso}} = \frac{Q_{\text{feed}}}{uD_t} = \frac{\pi d^2}{4D_t}U. \tag{11}$$

The micromixing time is determined as (Baldyga & Bourne, 1989)

$$\tau_{\text{micro}} = \frac{1}{E} \tag{12}$$

and hence

$$Q = \frac{EQ_{\text{feed}}}{uD_t}. \tag{13}$$

The turbulent diffusivity, D_t, can be estimated by (Baldyga & Bourne, 1999; Versteeg & Malalasekera, 1995)

$$D_t = \frac{\nu_t}{Sc_t} = \frac{C_\mu k^2}{Sc_t \varepsilon} = 0.1\frac{k^2}{\varepsilon}, \tag{14}$$

where k is the turbulent kinetic energy. The fluid dynamics modelling constant, C_μ, is 0.09 (Versteeg & Malalasekera, 1995) and the value of the turbulent Schmidt number is commonly 0.9 (Baldyga & Bourne, 1999). From turbulence measurements in the turbine discharge stream the kinetic energy is estimated as (Lee & Yianneskis, 1998)

$$k = \tfrac{3}{2}(u')^2 = \tfrac{3}{2}(0.256\pi N_{\text{turb}} D_{\text{turb}})^2 \tag{15}$$

at the feed point. We only account for the turbine contribution to the kinetic energy and the energy dissipation rate in the calculation of D_t and E.

The mesomixing times according to Eq. (11) are significantly lower than the macroscale circulation times in the loop reactor. The longest mesomixing time is 0.53 s and the shortest macroscale circulation time is 2.2 s. The micromixing times according to Eqs. (12) and (9) are in the range 0.001–0.057 s. U is calculated by using the resultant bulk flow velocity as given by Eq. (3), in the denominator. U ranges from 0.01 to 2.2. As shown by Eq. (11), the rate of mesomixing increases with decreasing value of U. For all the loop reactor experiments, Q ranges from about unity to 8. Hence, both mesomixing and micromixing are important. The highest Q-values are found when the highest feed rates are used and in this case the influence of mesomixing is dominating. The lowest Q-values are found when the lowest feed rates are used and then the influence of mesomixing and

micromixing is about equal. This explains why there is a significant influence of the feed pipe diameter and the feed rate over the whole range of our experiments.

Eq. (11) shows that the rate of mesomixing is expected to increase with increasing linear bulk flow velocity and with decreasing volumetric feed flow rate. In our experiments the weight mean size increases with increasing bulk flow velocity and with increasing total feed time, and the interpretation is that the mean size increases with increasing mixing intensity. Increased turbine agitation increases the rate of micromixing at the feed point as well as the rate of mesomixing via the influence on u_{res}, and this explains why the mean size increases with increasing turbine agitation rate. Experiments have been carried out in which the colour methyl violet was added through the different feed pipes to circulating water in the loop reactor at conditions equal to those of the crystallization experiments. By increasing the propeller agitation the coloured feed plume is axially more stretched out and we find it reasonable to assume that the scale of segregation decreases. Hence, the feed is mixed more efficiently with a larger volume of bulk solution. By increasing the turbine agitation, the coloured feed plume is radially and tangentially more stretched out and again the colouring experiments visualise that the feed can be expected to be more efficiently mixed with the bulk.

At very short times the exponential term in Eq. (5) becomes negligible and $X^0_{\mathrm{feed}} = U$. At very long times the argument of the exponential term approaches zero and if it is expanded into a Taylor series it can be shown that $X^0_{\mathrm{feed}} \propto Q/\sqrt{\varepsilon}$. However, as shown in Figs. 14 and 15, the results do neither correlate strongly with U nor with $Q/\sqrt{\varepsilon}$. In Fig. 14 the experimental data align linearly with the ratio U for each feed pipe diameter. The appearance of the figure resembles that of Fig. 13. Also in Fig. 15 the influence of the feed pipe diameter can be clearly distinguished.

In our results the weight mean size increases quite clearly with decreasing feed pipe diameter. Since increasing propeller agitation and increasing turbine agitation lead to increasing weight mean size we do find it reasonable to conclude that decreasing feed pipe diameter leads to improved mixing. However, this is contradictory to one of the key conclusions in the work of Baldyga et al. (1993). They found in experiments on a case with two parallel chemical reactions that the rate of mesomixing decreases when the feed pipe diameter decreases at constant total feeding time. They also found this conclusion to be supported by Eq. (5). By adding a coloured feed to water in the loop reactor we may observe that the feed is more difficult to mix when the feed rate increases for a particular feed pipe. However, for a particular volumetric feed rate we cannot observe a difference in the rate of mixing depending on the feed pipe diameter.

The relation between U and d in Eq. (6) inserted into Eq. (5) leads to the conclusion that mesomixing becomes

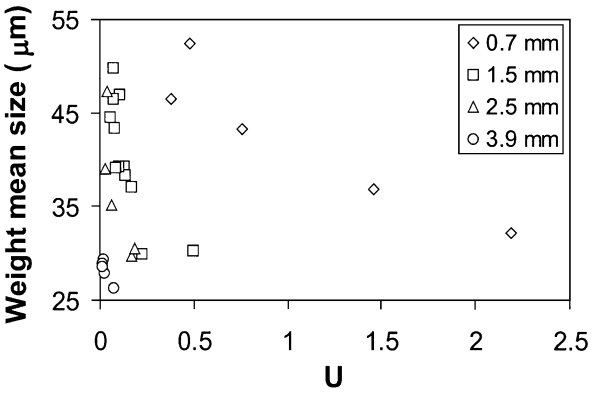

Fig. 14. Correlation of mean size to the dimensionless number U.

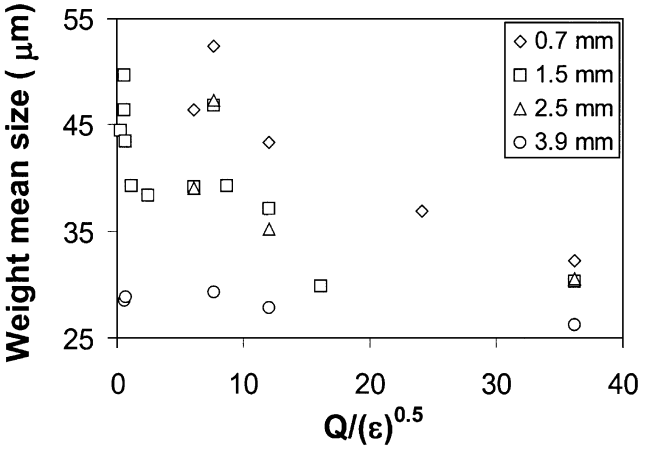

Fig. 15. Correlation of mean size to the number: $Q/\sqrt{\varepsilon}$.

faster at increasing feed pipe diameter at constant feeding time. The feed pipe diameter is also found in the argument of the exponential term. However, here the origin is different and in this position an increasing feed pipe diameter contributes to reduced mixing. Mathematically, U originates from the initial condition of the problem, i.e.

$$X_{\mathrm{feed}}[t=0] = U = \frac{4Q_{\mathrm{feed}}}{\pi d^2 u}. \tag{16}$$

The physical consequence of the initial condition is that the feed is immediately, at the exit of the feed pipe, homogeneously mixed with a certain amount of bulk solution, and after that further mixing occurs by turbulent diffusion. This seems to be an unrealistic assumption. The initial value is unity if the linear bulk flow velocity equals the linear velocity in the feed pipe. However, if $u_f > u$ (which, in fact, often is the case in the experiments used by Baldyga et al. (1993) to illustrate that the mesomixing increases with increasing feed pipe diameter) the initial volume fraction exceeds unity. At constant volumetric flow rate, the initial value, being equal to U, decreases with increasing feed pipe diameter. Hence

X^0_{feed} decreases, i.e. the rate of mesomixing increases. However, we may note that according to the definition, Eq. (11), the mesomixing time constant does not depend on the feed pipe diameter at constant volumetric flow rate.

The initial condition in the model describes the initial volume fraction of the feed solution at the entrance into the bulk solution. Baldyga et al. (1993) assumed that

$$X_A(t=0) = \frac{Q_{\text{feed}}}{Q_{\text{bulk}}} = \frac{u_{\text{feed}} d^2}{u d_b^2} \tag{17}$$

and defined as $d_b = d$. The reason for using Eq. (17) and the feed pipe diameter for d_b is not clear and is neither obvious from a physical point. The conditions are likely to depend on the value of U, i.e. at low U the feed behaves quite differently when it enters the bulk than at high U. In our experiments, U is lower or much lower than unity, except for a few cases. In the experiments of Baldyga et al. (1993), referred to above, the value of U exceeds unity in most cases. In fact in their experiments the feeding rate and the feed pipe linear velocity are almost an order of magnitude higher than in our work. Instead of using $d_b = d$ we may consider using the macroscale of the bulk flow turbulence which is then determined by the two agitators. In that case d_b is larger than d, and with no direct relation to the feed pipe diameter. We may also consider a length scale dependent on the additional turbulence that is generated by the feed pipe positioned in the bulk flow. In that case we would use a quantity related to the outer diameter of the feed pipe. In our work, the outer diameter is equal to 6 mm for all feed pipes except the 1.5 mm feed pipe diameter, where the outer diameter is equal to 3 mm. If U becomes independent of the internal diameter of the feed pipe, the rate of mesomixing according to Eq. (5) will decrease with increasing internal feed pipe diameter due to the argument of the exponential term.

Eq. (17) can be completely replaced, if we assume that the feed solution accelerates to the velocity of the bulk immediately at the exit and the cross-sectional dimensions change accordingly to fulfil a mass balance over the amount of feed. The initial value is unity, i.e. initially the feed consists of undispersed feed solution. However, the dimension of the feed flow attained immediately at the outlet, d_f, replaces the feed pipe diameter in the argument of the exponential term. The dimension, d_f, will depend on the relation between the flow inside the pipe and the bulk flow outside the pipe, and we may also include a dependence on the angle of the feed pipe to the bulk flow. However, by this approach we cannot find support for why mesomixing would increase with decreasing feed pipe diameter. In addition, experimental results show that the crystal mean size is almost independent of the feed pipe direction for the circular feed pipes and of the rotation orientation of the rectangular feed pipe. There is a quite strong effect of changing the shape of the feed pipe. The rectangular feed pipe behaves approximately as a circular feed pipe having a diameter equal to the shortest dimension of the rectangle. This suggests that the size and the shape of the feed pipe do influence the scale of segregation at the feed point. So far, the conclusion is that it cannot be shown that the turbulent dispersion model is able to describe the conditions in the present work. Our results suggest that the scale of segregation of the feed increases with increasing feed pipe dimensions.

4.3. Inertial-convective disintegration

Besides turbulent dispersion also inertial convective disintegration of large eddies may contribute to mesomixing (Baldyga et al., 1997). By this mechanism the scale of segregation is reduced by inertial forces from the integral scale of fluctuations, Λ, towards the Kolmogoroff microscale. The time constant for this mesomixing mechanism is given by

$$\tau_{\text{meso}} = A\left(\frac{\Lambda^2}{\varepsilon}\right)^{1/3}, \tag{18}$$

where the value of the constant A can be taken as 2. Different suggestions for estimation of the macroscale are given. One alternative is to use d_f as given by Eq. (19):

$$d_f = \sqrt{\frac{4Q_{\text{feed}}}{\pi u}} \tag{19}$$

which is based on the assumption that the feed is strained by the bulk flow. Another suggestion is to use $\Lambda = d$. This latter assumption, as opposed to the first, would lead to increased rate of mesomixing when decreasing the feed pipe diameter. However, it is claimed (Baldyga et al., 1997) that this assumption lacks experimental verification and that it does not account for the rate of mesomixing dependence on the volumetric feed flow rate. The model of mesomixing by inertial convective disintegration in a semibatch reactor states that the volume expansion of feed lumps follows an exponential function (Baldyga et al., 1997)

$$V_t = V_0 \exp\left(\frac{t}{\tau_{\text{meso}}}\right), \tag{20}$$

where V_0 is the initial volume of a feed lump. No guidelines for how V_0 may depend on processing conditions are given. We may speculate in a dependence where V_0 would increase with increasing feed pipe diameter. However, at present, we conclude that there is not a clear support in this theory for that mesomixing will increase with decreasing feed pipe diameter.

4.4. Feed point location

In a few additional experiments with the 0.7 mm feed pipe diameter we have examined the influence of the distance between the feed pipe and the tip of the turbine. The results from the experiments with a total feeding time of 30 min are presented in Fig. 16. The weight mean size increases quite strongly with decreasing distance to the turbine tip. This, further supports that increased mixing leads to increased crystal weight mean size. In addition this may provide an explanation for the influence of the feed pipe diameter. At constant volumetric flow rate the linear feed velocity increases with decreasing feed pipe diameter. Possibly, the feed flow penetrates somewhat closer to the turbine tip before being swept away by the bulk flow and the effect will be like moving the feed location closer to the turbine. If this explanation is important we would expect a similar effect of increasing the volumetric flow rate. However, an increasing feed rate, i.e. reduced feeding time always results in a reduced weight mean size. In addition, this very strong effect of the exact location is only seen for the smallest feed pipe at the shortest feeding time. When the total feeding time is increased to 90 min, the influence of the turbine agitation rate is strongly reduced. We tend to conclude that the prime variable is not the linear velocity in the feed pipe. Instead the pipe diameter and the volumetric flow rate is determining.

4.5. Feed pipe backmixing

Feed pipe backmixing can take place and has been observed visually both during the crystallizations and in the colouring experiments previously described. Backmixing into the feed pipe has been reported to decrease the mixing (Bourne, Kozicki, Moergeli, & Rys, 1981) and the influence of agitator type, agitation rate and feed point location on backmixing into a 9.5 mm feed pipe has been investigated (Fasano, Penney, & Xu, 1992). In the present study, backmixing was investigated by adding a colouring agent through the feed pipe. The influence of volumetric feed flow rate and turbine stirring rate was investigated, and the ratio of the linear feed velocity, u_{feed}, to the impeller tip speed, u_{tip}, is used to characterise the conditions. Backmixing (observed as colourless water being pushed into the feed pipe) is found for $u_{\text{feed}}/u_{\text{tip}} \leqslant 0.2$–$0.25$, which is somewhat higher than found by Fasano et al. (1992). In our work, backmixing is found at $N_{\text{turb}} = 75$ rpm for the 3.9 mm feed pipe already at $t_f = 30$ min, for the 2.5 mm feed pipe at $t_f \geqslant 90$ min and for the 1.5 mm feed pipe at first at 180 min feed time. The tendency for backmixing increases with increasing turbine stirring rate. However, in the crystallization experiments, the positive effect on the product weight mean size, of decreasing the feed pipe diameter, is not limited to low feed velocities and large feed pipes. Actually, the results for the 3.9 mm feed pipe do behave in a different way than the results for all other feed pipes, see Figs. 5–8. In fact, during the crystallization experiments severe backmixing is only observed for the 3.9 mm feed pipe and in all experiments with this feed pipe except for that at the shortest feed time. Furthermore, the way other process parameters influence the product mean size do not lend support to a hypothesis that backmixing is a dominating phenomenon that may explain the influence of the feed pipe diameter on the product weight mean size. Backmixing should increase with increased feeding time, increased turbine agitation and reduced distance to the turbine agitator, and accordingly such changes should lead to smaller crystals. In fact, increased feeding time and increased turbine agitation always result in larger crystals. This is in sharp contrast to the results of Bourne et al. (1981), who found that when feed pipe backmixing reduced the overall rate of mixing, an increased agitation rate and an increased reactant feed velocity also reduced the mixing.

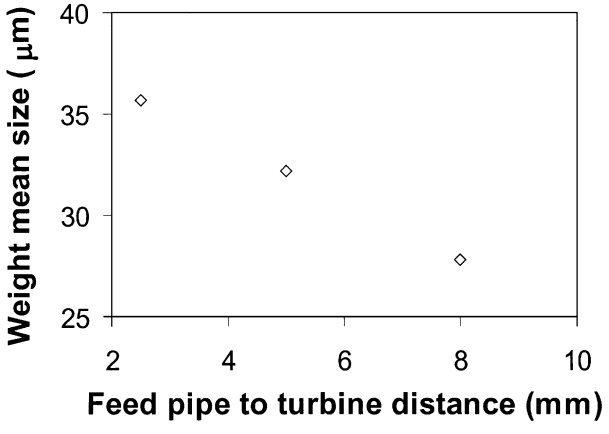

Fig. 16. Influence of the distance between the turbine impeller tip and the feed pipe, $d = 0.7$ mm, $t_f = 30$ min.

4.6. A new correlation

Different parameters for correlating the results have been tested quite extensively. It has been found that all data can be quite well correlated by a dimensionless number, TR, which can be interpreted as the ratio of the feeding time to the mixing time:

$$TR = \frac{t_f}{\tau_{\text{mix}}}. \tag{21}$$

Since the Q-value ranges from unity to about 8 it is expected that the overall mixing time is influenced by both mesomixing and micromixing and should be defined as

$$\tau_{\text{mix}} = \tau_{\text{meso}} + \tau_{\text{micro}}. \tag{22}$$

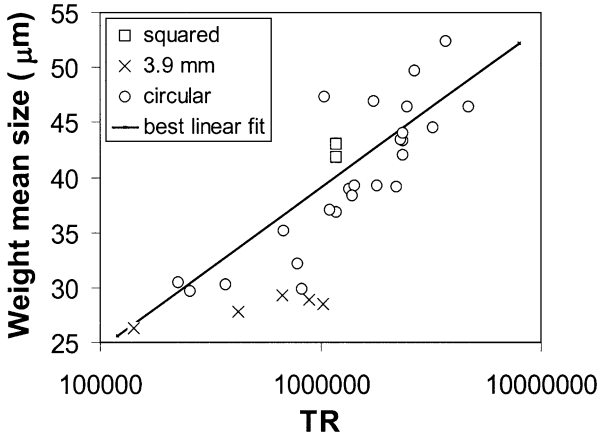

Fig. 17. Correlation of mean size to the dimensionless number, TR.

It has been found that the correlation is only successful if the time constant for mesomixing is defined differently than has been suggested previously by others. We have found that the ratio of the feed pipe diameter to the linear velocity of the flow passing the feed pipe outlet captures very much of the features of our results and in particular that the rate of mesomixing decreases with increasing internal diameter of the feed pipe. However, the magnitude of this ratio is at least one order of magnitude lower than the values obtained by Eqs. (11) and (18). Hence, as a first step we introduce an empirical parameter K which in addition is used to obtain the best fit between TR and the experimental weight mean sizes. Hence, the mesomixing time constant is defined as

$$\tau_{\text{meso}} = K\frac{d}{u_{\text{res}}}. \tag{23}$$

In spite of the Q-values it turns out that the best correlation is obtained if K is so large that the micromixing term becomes negligible and TR can be calculated simply as $TR = t_f u_{\text{res}}/d$. This correlation is shown in Fig. 17. However, the turbine contribution in u_{res} is somewhat approximate and if the tangential contribution is neglected a certain influence of the micromixing term can be observed.

A few points do not fall well into the overall correlation. Four of these data points are for the largest feed pipe: 3.9 mm. For this feed pipe, backmixing is strong and the product mean size is determined by mechanisms that are not captured by TR. Two of the others represent experiments being slight outliers already in the results presentation diagrams, e.g. 450 rpm (1.5 mm i.d.) and 900 rpm (2.5 mm i.d.) propeller stirring rates at 75 rpm turbine stirring rate in Fig. 5. As shown in Fig. 17 the results from the rectangular feed pipe are well correlated when the smallest dimension of the feed pipe is used as a characterising dimension in Eq. (23). In Fig. 17 we have also drawn a best-fitted straight line for all data points, except for those where the feed pipe diameter is 3.9 mm. The coefficient of correlation is 0.86.

5. Conclusions

The influence of different levels of mixing on the product weight mean size in semi-batch reaction crystallization, has been investigated. Benzoic acid was crystallized by mixing hydrochloric acid into an aqueous solution of sodium benzoate. A loop reactor is used to simulate the conditions in an agitated tank crystallizer. A marine propeller controls the macroscale circulation flow and a turbine agitator controls the feed point mixing intensity. The experimental results clearly show that the product weight mean size increases with increased macroscale circulation rate and increased feed point mixing intensity. In addition, the weight mean size increases with reduced feed rate and decreased feed pipe diameter. The process is mainly governed by mesomixing.

Available mesomixing models can explain the observed influence of the feed flow rate and of the macroscale circulation rate. However, the influence of the feed pipe diameter is quite opposite to predictions by available theories of mesomixing. In the present study, decreasing feed pipe diameter leads to increasing weight mean size at constant volumetric flow rate. In comparison to the influence of other process variables, this strongly suggests that the rate of mesomixing increases with decreasing pipe diameter. This effect of the feed pipe diameter cannot be explained by backmixing into the feed pipe. Backmixing is observed in the largest feed pipe. However, in the influence of the marine propeller agitation rate, the turbine agitation rate and the volumetric feed flow rate, there is no support for that backmixing is a dominating phenomenon that may explain the feed pipe diameter effect on the product weight mean size.

A dimensionless parameter, TR, is defined by which all experimental results are correlated quite well. TR is equal to the ratio of the total feeding time and the mixing time; the mixing time is defined as the sum of the time constants for mesomixing and micromixing. The mesomixing time constant is defined as being directly proportional to the ratio of the feed pipe diameter and the bulk flow velocity.

Notations

A	constant, dimensionless
C_μ	computational fluid dynamics modelling constant, dimensionless
d	feed pipe diameter, m
d_b	"diameter of bulk flow" passing the feed pipe (Eq. (17)), m
d_f	characteristic feed plume dimension, m

D diameter of impeller, m
D_t turbulent diffusivity, m^2/s
D_{turb} diameter of turbine, m
E engulfment rate coefficient, s^{-1}
k turbulent kinetic energy, m^2/s^2
K empirical constant used in Eq. (23), dimensionless
L_D characteristic length scale of mesomixing, m
L_i crystal size of size interval i, m
L_{43} weight mean size, m
N stirring rate, rps
N_i number of particles in size interval i, dimensionless
N_p power number, dimensionless
N_{prop} propeller agitation rate, rps
N_{turb} turbine agitation rate, rps
P average specific energy dissipation, W/kg
Q ratio of characteristic times of meso- and micromixing, dimensionless
Q_{bulk} volumetric bulk flow, m^3/s
Q_{feed} volumetric feed flow, m^3/s
Sc_t turbulent Schmidt number, dimensionless
t time since the feed left the feed pipe, s
t_f total feeding time, s
T dimensionless time, dimensionless
TR dimensionless number defined in Eq. (21), dimensionless
u velocity, m/s
u' fluctuating velocity, m/s
u_b measured linear bulk velocity in the loop reactor ($= 1.05/t_c$), m/s
u_{feed} linear velocity in the feed pipe, m/s
u_r radial mean velocity from the turbine impeller, m/s
u_{res} resultant velocity passing the feed point, m/s
u_t tangential mean velocity from the turbine impeller, m/s
u_{tip} turbine impeller tip speed, m/s
U ratio of linear feed velocity and bulk velocity, dimensionless
V_0 initial volume of feed lump, m^3
V_t volume of fluid containing the added reactant, m^3
X^0_{feed} initial volume fraction of A at feed pipe entrance, dimensionless

Greek letters

ε local energy dissipation, W/kg

Λ macroscale turbulence, m
ν kinematic viscosity, m^2/s
ν_t turbulent kinematic viscosity, m^2/s
ρ density, kg/m^3
τ_{meso} characteristic mesomixing time, s
τ_{micro} characteristic micromixing time, s
τ_{mix} characteristic mixing time, s

Acknowledgements

The financial support of the Swedish Research Council for Engineering Sciences (TFR) and the Swedish Industrial Association for Crystallization Research and Development (IKF) is gratefully acknowledged.

References

Åslund, B., & Rasmuson, Å. C. (1992). Semibatch reaction crystallization of benzoic acid. *A.I.Ch.E. Journal*, *38*, 328–342.

Baldyga, J., & Bourne, J. R. (1989). Simplification of micromixing calculations. I. Derivation and application of new model. *Chemical Engineering Journal*, *42*, 83–92.

Baldyga, J., & Bourne, J. R. (1992). Interactions between mixing on various scales in stirred tank reactors. *Chemical Engineering Science*, *47*, 1839–1848.

Baldyga, J., & Bourne, J. R. (1999). *Turbulent mixing and chemical reactions*. England: Wiley.

Baldyga, J., Bourne, J. R., & Hearn, S. J. (1997). Interaction between chemical reactions and mixing on various scales. *Chemical Engineering Science*, *52*, 457–466.

Baldyga, J., Bourne, J. R., & Yang, Y. (1993). Influence of feed pipe diameter on mesomixing in stirred tank reactors. *Chemical Engineering Science*, *48*, 3383–3390.

Baldyga, J., Podgorska, W., & Pohorecki, R. (1995). Mixing-precipitation model with application to double feed semibatch precipitation. *Chemical Engineering Science*, *50*, 1281–1300.

Baldyga, J., Pohorecki, R., Podgorska, W., & Marcant, B. (1990). Micromixing effects in semibatch precipitation. *Proceedings of 11th International Symposium on industrial crystallisation*, Garmisch-Partenkirchen, Federal Republic of Germany.

Bourne, J. R., Kozicki, F., Moergeli, U., & Rys, P. (1981). Mixing and fast chemical reaction – III. *Chemical Engineering Science*, *36*(10), 1655–1661.

Chen, J., Zheng, C., & Chen, G. (1996). Interaction of macro- and micromixing on particle size distribution in reactive precipitation. *Chemical Engineering Science*, *51*, 1957–1966.

David, R., & Marcant, B. (1994). Prediction of micromixing effects in precipitation: Case of double-jet precipitators. *A.I.Ch.E. Journal*, *40*, 424–432.

Fasano, J. B., Penney, W. R., & Xu, B. (1992). *Feedpipe backmixing in agitated vessels.* A.I.Ch.E. Symposium Series, vol. 293 (pp. 1–7).

Franke, J., & Mersmann, A. (1995). The influence of the operational conditions on the precipitation process. *Chemical Engineering Science*, *50*, 1737–1753.

Geisler, R. K. (1991). *Fluiddynamik und Leistungseintrag in turbulent gerührten Suspensionen.* Doctoral thesis, Munich, Germany.

Houcine, I., Plasari, E., David, R., & Villermaux, J. (1997). Influence of mixing characteristics on the quality and size of precipitated calcium oxalate in a pilot scale reactor. *Chemical Engineering Research and Design*, *75*, 252–256.

Kuboi, R., Harada, M., Winterbottom, J. M., Anderson, A. J. S., & Nienow, A. W. (1986). Mixing effects in double-jet and single-jet precipitation. *World congress III of chemical Engineering*, Tokyo, 8g-302 (pp. 1040–1043).

Lee, K. C., & Yianneskis, M. (1998). Turbulence properties of the impeller stream of a rushton turbine. *A.I.Ch.E. Journal*, *44*, 13–24.

Marcant, B., & David, R. (1991). Experimental evidence for and prediction of micromixing effects in precipitation. *A.I.Ch.E. Journal*, *37*, 1698–1710.

Marcant, B., & David, R. (1993). Influence of micromixing on precipita tion in several crystallizer configurations. *Proceedings of 12th international symposium on industrial crystallisation*, Warsaw, Poland (pp. 2-021–2-026).

Muhr, H., David, R., Villermaux, J., & Jezequel, P. H. (1995). Crystallization and precipitation engineering – V. Simulation of the Precipitation of silver bromide octahedral crystals in a double-jet semibatch reactor. *Chemical Engineering Science*, *50*, 345–355.

Nienow, A. W. (1985). In N. Harnby, M. F. Edwards, A. W. Nienow (Eds.), *Mixing in the process industries*. London, Great Britain: Butterworths.

Oldshue, J. Y. (1983). *Fluid mixing technology*. New York, NY, USA: McGraw-Hill Publications Co.

Philips, R., Rohani, S., & Baldyga, J. (1999). Micromixing in a single-feed semi-batch precipitation process. *A.I.Ch.E. Journal*, *45*, 82–92.

Podgorska, W., Baldyga, J., & Pohorecki, R. (1993). Micromixing effects in double feed semibatch precipitation. *Proceedings of 12th international symposium on industrial crystallisation*, Warsaw, Poland (pp. 2-015–2-020).

Ramsden, J. J. (1985). Nucleation and growth of small CdS aggregates by chemical reaction. *Surface Science*, *156*, 1027–1039.

Randolph, A. D., & Larson, M. A. (1988). *Theory of particulate processes.* (2nd ed.). New York, USA: Academic Press.

Rushton, J. H., Costich, E. W., & Everett, H. J. (1950). Power characteristics of mixing impellers — Parts I and II. *Chemical Engineering Progress*, *46*, 395–467.

Stavek, J., Fort, I., Nyvlt, J., & Sipek, M. (1988). Influence of hydrodynamic conditions on the controlled double-jet precipitation of silver halides in the mechanically agitated system. *Proceedings of sixth European conference on mixing*, Pavia, Italy (pp. 171–176).

Torbacke, M. (1998). *Reaction crystallisation — analysis of a semibatch process*. Licentiate thesis, Royal Institute of Technology, Stockholm, Sweden.

Tosun, G. (1988). An experimental study of the effect of mixing on the particle size distribution in $BaSO_4$ precipitation reaction. *Proceedings of the sixth European conference on mixing*, Pavia, Italy (pp. 161–170).

Tovstiga, G., & Wirges, H. -P. (1990). The effect of mixing intensity on precipitation in a stirred tank reactor. *Proceedings of 11th international symposium on industrial crystallisation* Garmisch-Partenkirchen, Federal Republic of Germany (pp. 169–174).

Versteeg, H. K., & Malalasekera, W. (1995). *An introduction to computational fluid dynamics — the finite volume method*. England: Longman Scientific & Technical.

Wu, H., & Patterson, G. K. (1989). Laser Doppler measurements of turbulent flow parameters in a stirred mixer. *Chemical Engineering Science, 44*.